J Seismol (2007) 11:199–204
DOI 10.1007/s10950-007-9047-1

ORIGINAL ARTICLE

Estimation of velocity in the uppermost crust in a part of the western Gulf of Corinth, Greece, from the inversion of *P* and *S* arrival times using the neighbourhood algorithm

Jaromír Janský · Vladimír Plicka · Helene Lyon-Caen · Oldřich Novotný

Received: 2 May 2006 / Accepted: 24 January 2007 / Published online: 1 March 2007

Abstract We determine the velocities in an upper crustal model, composed of three homogeneous layers, for one subregion of the western part of the Gulf of Corinth, NE of the town of Aigion, Greece. We have used local events that occurred there in the year 2001 and were recorded by the Corinth Rift Laboratory Network. Weighted *P* and *S* arrival time residuals are minimized using the Neighbourhood Algorithm of Sambridge (1999), combined with the grid search for source locations. The resolution of the inversion is tested by delete-one jackknifing. The model obtained is compared with some other models derived or applied to the subregion. A fast velocity increase between depths of 5 and 7 km is confirmed as the major structural element.

Keywords Uppermost crust · Gulf of Corinth · Arrival times · Inversion · Neighbourhood algorithm

J. Janský (✉) · V. Plicka · O. Novotný
Faculty of Mathematics and Physics, Charles University, Prague, Czech Republic
e-mail: jansky@seis.karlov.mff.cuni.cz

H. Lyon-Caen
Laboratory de Géologie, Ecole Normale Supérieure, Paris, France

1 Introduction

The western part of the Gulf of Corinth is very active seismically. Interesting geodynamic processes and the related seismic hazard call for detailed studies of this area. Therefore, in addition to standard monitoring (of stronger events) of this area by the all-Greece seismic network of the National Observatory of Athens, NOA (see: http://www.gein.noa.gr), and the western Greece network of the University of Patras, PATNET (see: http://seismo.geology.upatras.gr), special seismic studies are carried out in this area using temporary seismic networks. In particular, detailed investigations have been accomplished as part of the Corinth Rift Laboratory (CRL) Project. For this purpose, the CRL seismic network (CRLNET) was deployed on the northern and southern coasts of the Gulf of Corinth (Lyon-Caen et al. 2004).

For event location, the CRL uses a layered structural model, hereinafter referred to as CRLM. This model resulted from a seismological experiment carried out in 1991 (Rigo et al. 1996) when 51 digital seismic stations (30 of them three-component stations) covered a territory of 45×45 km of the western part of the Gulf. This territory is centred approximately at 22.0°E and 38.35°N (the Psathopyrgos–Aigion area), which is roughly delineated by the frame in Fig. 1. The CRLM is an average 1-D model composed of six homogeneous layers over a homogeneous halfspace with the MOHO at a depth of

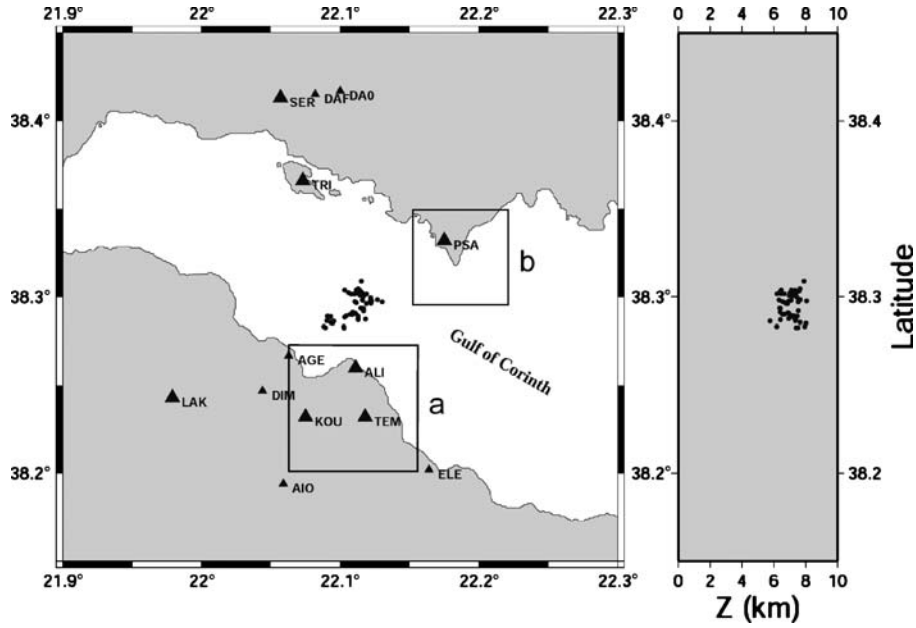

Fig. 1 The western part of the Gulf of Corinth with epicentres and depths of the set of 55 events from the 2001 CRLNET catalogue (dots). Triangles denote the 13 stations that recorded at least some of these events. Large triangles are the seven stations that were used for the inversion. The two squares give the positions of subregions a) and b) from the tomography study of Latorre et al. (2004)

30 km. The v_P/v_S velocity ratio is 1.80. The top 18 km of this model is shown in Fig. 2.

The 1991 experiment data have recently been inverted into a 3-D tomography model of this area (Latorre et al. 2004). The CRLM was used as the 1-D "minimum velocity model" for that task (Kissling et al. 1994). The results for five subregions of the area were presented in the form of 1-D velocity sections for depths ranging from 2 to 13 km; see Latorre et al. 2004, page 1029, Figure 16. Subregions a) and b) in this figure, delineated in our Fig. 1, have similar v_P velocity sections. They can be roughly approximated by three layers with constant velocity gradients with the layer bottoms at depths of 5, 7 and 13 km, respectively. The second layer has a larger velocity gradient than the other two. The average of these two velocity sections is shown in Fig. 2 as the TM (tomographic) model.

Several thousands of events were recorded by the CRLNET during the year 2001. A significant part of them was located by HYPO (Lee and Valdés 1989) using the CRL model, in the vicinity of subregions a) and b). These events are situated in the subregion whose centre is near to 22.1°E and 38.3°N. The proximity of these events to subregions a) and b) makes it possible to use the data of these events for determining a local model of the upper crust. The purpose is to compare the results with that of the tomography for this subregion (TM model) and also with CRLM, which represents an average model for a much broader area.

To be able to use our local model for the HYPO location, we looked for a model composed of homogeneous layers. In accordance with the layering of the TM model, we have also limited ourselves to just three layers and have further adopted the layer thicknesses of the TM model as a priori information for the present study. Hence, we only invert the velocities.

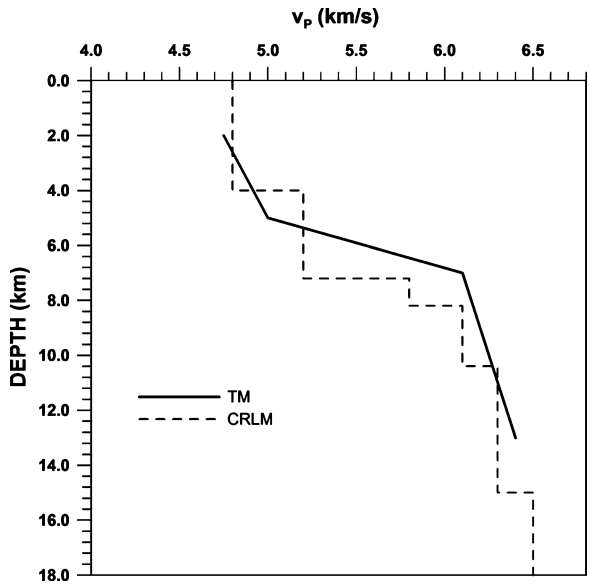

Fig. 2 1-D velocity models: TM is the average model from tomography for subregions a) and b) shown in Fig. 1. CRLM is the model used for HYPO locations by the Corinth Rift Laboratory (Rigo et al. 1996)

Table 1 Total of *P* and *S* waves weights of the 55 events at individual stations

Station	Number of events	Sum of *P* weights	Sum of *S* weights
Southern coast stations			
ALI	35	29.75	19.00
KOU	55	41.75	15.50
TEM	54	47.25	19.25
LAK	50	50.00	22.50
Northern coast stations			
PSA	55	54.00	28.00
TRI	55	55.00	27.25
SER	46	35.25	23.50

For the present study, we have selected a set of 55 events (dots in Fig. 1) of the mentioned events, satisfying the following conditions: (1) Each event had a magnitude of two or greater, (2) it was recorded at least at six stations, of these at least two stations were situated on the northern coast and at least three stations were situated on the southern coast. These events were recorded at different stations of the CRL network (a total of 13 stations were involved, see triangles in Fig. 1). However, only stations ALI, LAK, KOU and TEM on the southern coast, and PSA, TRI and SER on the northern coast (see large triangles in Fig. 1) recorded more than 1/5 of the 55 events. Consequently, we further used only the data from these seven stations (Stations SER and LAK are operated by agencies other than CRL, but their data are supplied to CRL).

2 Inversion of data

2.1 Method

Many different techniques can be used to derive a structural model from arrival times, such as genetic algorithms (Holland 1975), isometric inverse algorithm (Málek et al. 2005), etc. We have selected the Neighbourhood Algorithm (NA) method (Sambridge 1999) because in highly non-linear space, it has more 'power' to escape from local minima than, for example, genetic

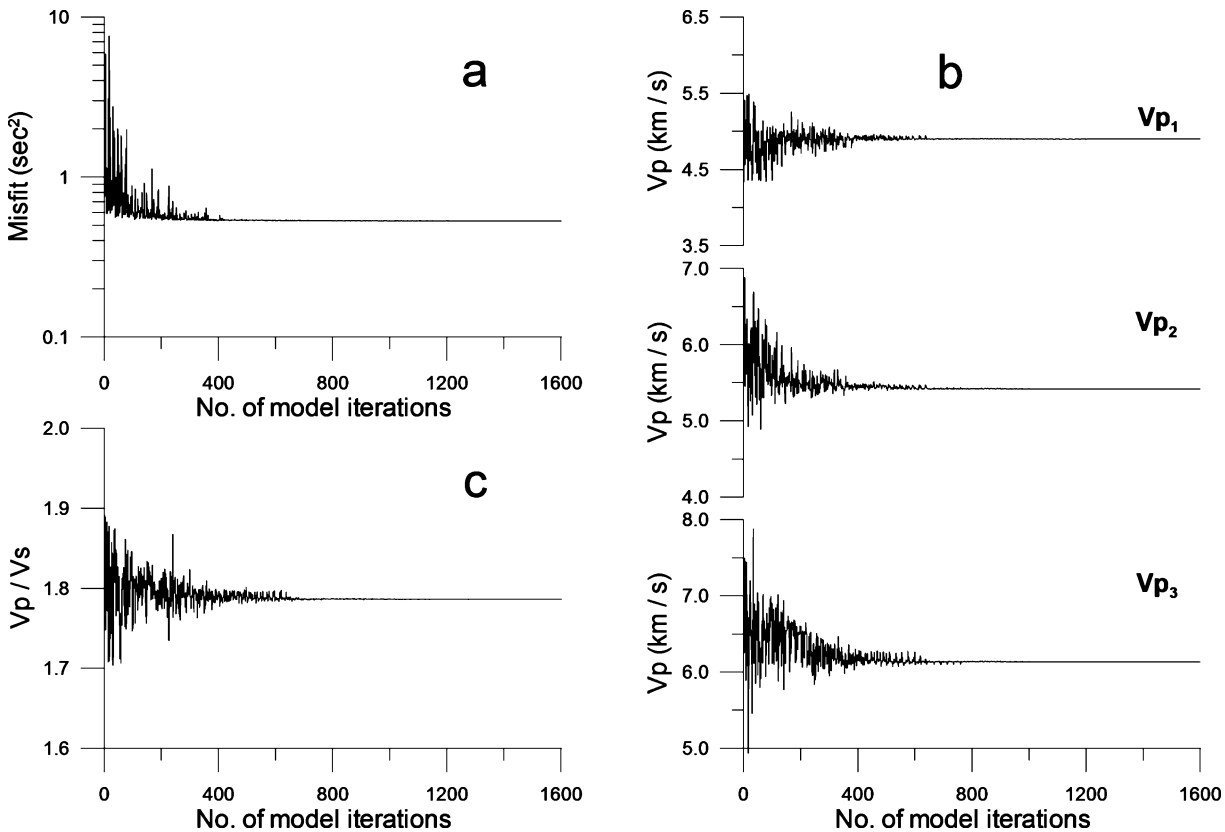

Fig. 3 Convergence of the individual parameters, using the NA algorithm: (**a**) misfit function, (**b**) v_{P1}, v_{P2} and v_{P3}, (**c**) v_P/v_S

Table 2 Individual inverted parameters and their standard deviation

v_P/v_S	v_{P1} (km/s)	v_{P2} (km/s)	v_{P3} (km/s)
1.79±0.06	4.90±0.24	5.42±0.23	6.13±0.35

algorithms (Valleé and Bouchon 2004; Sambridge 1999; Lomax and Snieder 1994). The main idea of the NA is the following: for each point in parameter space (i.e. for each combination of the model parameters), it is assumed that, to a first approximation, the fit is constant in some neighbourhood. To describe the neighbourhood, Voronoi cells are used (Voronoi 1908). They are defined in the space of all searched parameters; they are unique and define a convex, space-filling pavement of the space. Sambridge then describes the NA as follows: (1) generate an initial set of *ns* models, each model being a certain combination of model parameters; (2) calculate the misfit function for the (most recently generated) set of *ns* models and determine the *nr* models with the lowest misfit of all models generated so far; (3) generate *ns* new models by performing a uniform random walk in the Voronoi cell of each of the *nr* choosen models (i.e. *ns*/*nr* samples in each cell); (4) go to step 2.

2.2 Conditions of inversion

In our experiments, we have 654 data (350 *P*-wave and 304 *S*-wave onsets), weighted by the observers (Lee and Valdés 1989), and search for four structural parameters: the v_P/v_S ratio and v_P velocities in the three layers. To be able to exclude low-velocity layers, we invert the velocity increase dv_{Pi+1}, where $v_{Pi+1} = v_{Pi} + dv_{Pi+1}$, in the second and third layer rather than the velocity itself (The thicknesses of the layers are the same as in the tomographic model). The constant v_P/v_S ratio simplifies the inversion numerically. Due to the significantly lower total weight of the *S* waves, 155.00, as compared with the 313.00 for the *P* waves, we do not expect the influence of the constant v_P/v_S to be critical. The weights of the data of the southern stations, 168.75 for the *P* waves and 76.25 for the *S* waves, are comparable with the weights of data of the northern stations, 144.25 for the *P* waves and 78.75 for the *S* waves. For statistics, see Table 1. We use $ns=20$, $nr=10$, and the total number of iterations of 80, i.e. a total of 1,600 crustal models are generated by the NA.

We define the misfit function as the sum of the weighted arrival-time residuals (L2 norm) of the *P* and *S* waves over all stations and hypocentres of all the events. The location is done by grid search where the rectangular 3-D location grid covers roughly an area of 55 hypocentres with a step of 0.2 km in all three directions. To illustrate the performance of the NA, we show the convergence of the misfit function of v_{P1}, v_{P2}, v_{P3} and of v_P/v_S in Fig. 3. It appears that about half of the used iterations would be sufficient to get the inversion.

2.3 Results

The individual parameters v_{P1}, v_{P2}, v_{P3} and v_P/v_S, obtained from the inversion, are given in Table 2. To get their standard deviation, we run the inversion again seven times, each time omitting the data from one of the seven stations (delete-one jackknifing, Tichelar and Ruff 1989). The obtained standard deviations are also given in Table 2.

The v_P velocities in the three-layered model (denoted as the M55 model), obtained from the inversion, are in Fig. 4 compared with the average

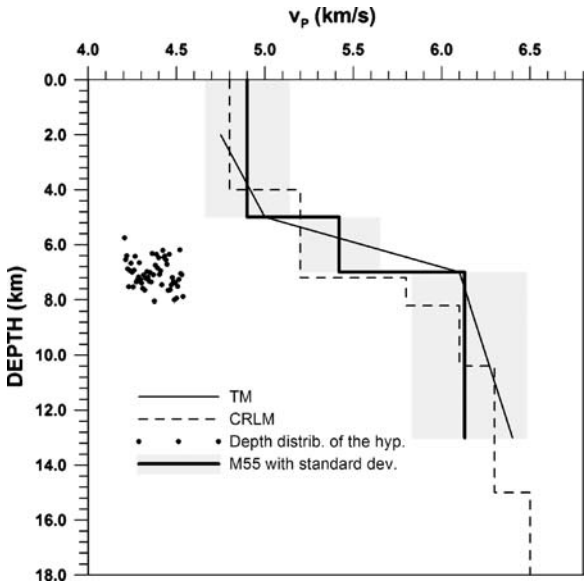

Fig. 4 *P*-wave velocities in the individual layers of the M55 model, derived in the present study (solid line). The shaded zone gives their standard deviation obtained by delete-one jackknifing. The average tomography model TM and the CRLM model are shown for comparison. The group of dots represent the depth distribution of the hypocentres of events, located by the HYPO code in the CRLM model (The coordinate in the horizontal axis for dots is arbitrary)

tomographic TM model and CRLM model. The M55 model velocities follow roughly the TM model velocities in the upper two layers, but are lower in the third layer. The standard deviation in the third layer is higher than those for the two upper layers. This is due to the fact that only a part of the events is located in the third layer, and the waves from the rest of events do not propagate through this layer. If compared with the CRLM velocities, the M55 model velocities in the first two layers are slightly larger on average (of about 0.1 km/s).

The depths of our events lie in only a very narrow interval around 7 km (±1 km). Due to the lack of shallower hypocentres, the resolution of the inversion must be expected to be low although we have determined only a small number of structural parameters, namely only the velocities and not the layer thicknesses. This is reflected in the large standard deviations of the M55 model velocities. The concentration of most of the hypocentres in the rather narrow band of depths characterises even the data used in the tomography (Latorre et al. 2004). The large standard deviations are also due to the significant azimuthal gaps in events location, which follow from the mutual configuration of the seismic stations and epicentres area. The average gap value is 122°, the limits being 102° and 151°.

The comparison of the differences for the HYPO location in models CRLM and in M55 might be of interest. The average RMS for the CRLM is slightly smaller (0.044 s) than the RMS for the M55 model (0.048 s). The average difference in epicentres is 0.22 km, and the average difference in the depths is 0.28 km. The centre of the cluster of 55 events in the M55 model is shifted by 0.19 km to the east, 0.08 km to the south and is 0.25 km deeper, as compared with the location in the CRLM. The dispersion of the cluster is about the same, the mean deviation being 0.72 km in longitude, 0.68 km in latitude and 0.51 km in depth for the M55 location, as compared with 0.65 km in longitude, 0.67 km in latitude and 0.51 km in depth for the CRLM location.

3 Conclusion

The v_P depth distribution for the M55 model, derived in this study, generally follows the trend of the tomographic gradient model TM, obtained as the average of two nearby velocity sections from the tomography (Latorre et al. 2004). Therefore, considering that our approach makes use of different sources, stations and methods, the results of this paper complement the tomographic study in the particular subregion of the Gulf of Corinth.

The major structural element confirmed is the fast velocity increase between the depths of 5 and 7 km, as obtained by the tomography (Latorre et al. 2004) for the two neighbouring subregions. The lack of earthquake sources down to the depth of 5 km and rather large azimuthal gaps cause large standard deviations of velocities. The v_P/v_S ratio found (1.79) is within the limits of the v_P/v_S ratio from tomography (which oscillate roughly between 1.7 and 1.8 for the first subregion and between 1.65 and 1.85 for the second subregion—Latorre et al. 2004) and is very near to that of the CRLM (1.80).

The ‘quality’ of both the M55 and CRLM layered models for locating the events in the mentioned subregion using the HYPO code is about the same, although the CRLM was derived as the average model for a much larger area.

Acknowledgements We are grateful to three anonymous reviewers for their critical comments that led to substantial changes of the original manuscript. This work was partially supported by the EC project No. 004043-3HAZ-Corinth and research project GACR 202/04/P056 in the Czech Republic.

References

Holland JH (1975) Adaptation in natural and artificial systems. University of Michigan Press, Michigan

Kissling E, Ellworth WI, Eberhard-Phillips D, Kradolfer U (1994) Initial reference models in local earthquake tomography. J Geophys Res 99:19635–19646

Latorre D, Virieux J, Monfret T, Monteiller V, Vanorio T, Got J-L, Lyon-Caen H (2004) A new seismic tomography of Aigion area (Gulf of Corinth, Greece) from the 1991 data set. Geophys J Int 159:1013–1031

Lee WHK, Valdés CM (1989) Hypo71PC. Toolbox for seismic data acquisition, processing, and analysis. IASPEI & SSA

Lomax A, Snieder R (1994) Finding sets of acceptable solutions with a genetic algorithm with application to surface wave group dispersion in Europe. Geophys Res Lett 21:2617–2620

Lyon-Caen H, Papadimitriou P, Deschamps A, Bernard P, Makropoulos K, Pacchiani F, Patau G (2004) First results of the CRLN seismic array in the western Corinth rift: evidence for old fault reactivation. C R Geoscience 336:343–351

Málek J, Horálek J, Janský J (2005) One-dimensional qP-wave velocity model of the upper crust for the west Bohemia/Vogtland earthquake swarm region. Stud Geophys Geod 49:501–524

Rigo A, Lyon-Caen H, Armijo R, Deschamps A, Hatzfeld D, Makropoulos K, Papadimitriou P, Kassaras I (1996) A microseismic study in the western part of the Gulf of Corinth (Greece): implications for large scale normal faulting mechanisms. Geophys J Int 126:663–688

Sambridge M (1999) Geophysical inversion with a neighbourhood algorithm. I. Searching a parameter space. Geophys J Int 138:479–494

Tichelaar BW, Ruff LJ (1989) How good are our best models? Jackknifing, bootstrapping, and earthquake depth. Eos Trans AGU 70:593

Valleé M, Bouchon M (2004) Imaging coseismic rupture in far field by slip patches. Geophys J Int 156:615–630

Voronoi MG (1908) Nouvelles applications des paramètres continus à la théorie des formes quadratiques. J Reine Angew Math 134:198–287